JOURNAL OF GAS TECHNOLOGY

Volume 9 / Issue 2 / Winter 2024 / Pages 54-69

Journal Home page: http://jgt.irangi.org

Optimisation of Steel Pipe-Rack Structures in the Oil Industry Using Metaheuristic Algorithms

Ruholamin Chatrazar[1], Hamed Ghohani Arab[2*], Mahmoud Miri[3]

1. Master's student, Department of Civil Engineering, Faculty of Engineering, University of Sistan and Baluchestan, Zahedan, Iran
2. Associate Professor, Department of Civil Engineering, Faculty of Engineering, University of Sistan and Baluchestan, Zahedan, Iran
3. Professor, Department of Civil Engineering, Faculty of Engineering, University of Sistan and Baluchestan, Zahedan, Iran

ARTICLE INFO

ORIGINAL RESEARCH ARTICLE

Article History:
Received: 14 November 2024
Revised: 19 December 2024
Accepted: 30 December 2024

Keywords:
Steel pipe rack structure
Optimisation
Metaheuristic algorithms
Grey Wolf Optimiser (GWO) algorithm
Whale Optimisation Algorithm (WOA)

ABSTRACT

Steel pipe racks are among the most critical structures in various industries, including oil and petrochemical sectors. They are used for transporting fluids, gases, and chemicals. Given the extensive application of these structures in the oil and gas industry, their optimisation is of paramount importance. This research aims to reduce the construction costs of steel pipe racks via practical weight optimisation using the Grey Wolf Optimiser (GWO) and Whale Optimisation Algorithm (WOA) metaheuristic algorithms, as well as comparing their responses. In this study, the aforementioned algorithms are developed automatically through MATLAB, and by interfacing with ETABS, enable the optimal design of steel pipe racks while adhering to design code requirements. Leveraging metaheuristic algorithms and complying with design code requirements, this research seeks to provide a practical solution for the safe and optimised design of steel pipe rack structures, thereby reducing construction costs in the oil and gas industry. The proposed framework is evaluated on two steel pipe racks, incorporating key design considerations. The results demonstrate that both GWO and WOA metaheuristic optimisation methods can serve as effective tools for engineers in achieving cost-efficient designs.

DOR: 20.1001.1/jgt.2025.2057791.1055

How to cite this article
R. Chatrazar, H. Ghohani Arab, M. Miri, Comparative Study of Biotreated Leachate before and After Using AOPs Treatment for Removing COD, BOD and Color. Journal of Gas Technology. 2024; 9(2): 54-69. (https://www.jgt.irangi.org/article_725004.html)

* Corresponding author.
E-mail address: ghohani@eng.usb.ac.ir, (H. Ghohani Arab).

Available online 30 December 2024

1. Introduction

Given the growing global demand for energy, the oil and gas industry continues to play a pivotal role in meeting this need. According to forecasts by the International Energy Agency (IEA), oil consumption in Middle Eastern continues to constitute the majority of energy use. China, recognised as the world's largest petrochemical consumer, continues to exhibit rising demand. The expansion of petrochemical production in China has been a key driver of recent oil market shifts, altering the distribution of petrochemical outputs in other regions. Moreover, this trend has partially offset declining demand in other sectors. Between 2019 and 2023, China's oil consumption as petrochemical feedstock increased by over 1.5 million barrels per day. Over the next decade, oil demand growth in the country is expected to remain primarily driven by petrochemical industry development.

Meanwhile, in emerging and developing economies—home to the majority of the global population—energy demand has grown at an average annual rate of 2.6% over the past decade. This surge stems from factors such as population growth, a 50% expansion in economic output, and a 40% increase in industrial production. Additionally, built-up area has grown by 40,000 square kilometres, equivalent to the total land area of the Netherlands. Given this rapid development, clean energy in these economies must expend considerably more effort to replace fossil fuels—including oil, gas, and coal—compared to advanced economies(Agency International Energy, 2024). This high demand level underscores that oil and gas infrastructure in emerging economies requires urgent development.

Despite the development of renewable energy, oil will remain one of the world's primary energy sources, particularly in the Middle East, China, and India, which play a pivotal role in global production and consumption markets. The optimisation of pipe rack structures can be economically and environmentally justified under these circumstances. It may significantly enhance the productivity of the oil and gas industry. In this context, research on pipe rack structures can improve system performance and reduce operational costs. A key objective of this study is to identify and implement optimisation methods for designing pipe racks to reduce costs while maintaining the efficiency and safety of oil and gas condensate transportation. In recent years, limited research has been conducted on the optimisation of pipe rack structures. In 2010, Richard Drake and Robert Walter summarised design load codes and other design considerations for piperacks(M. DRAKE & J. WALTER, 2010). Karimi et al. (2011) evaluated the seismic performance of existing pipe racks in Iranian petrochemical plants(Karimi et al., 2011). In 2019, Kaval and Naval studied three bracing patterns in pipe racks to achieve an optimised configuration through positional adjustments(Kawade & Navale, 2019). Nitish J. Singh and Mohammad Eshtiaghi (2016) conducted an optimised design and analysis of steel pipe racks for gas industry in compliance with international codes and standards(J Singh & Ishtiyaque, 2016). Shahidtabar and Mirghaderi (2013) proposed a novel method to account for pipe-rack interaction, reducing material usage by 29%(Shahiditabat & Mirghaderi, 2013). Pooya Zakian et al. (2021) optimised steel pipe racks using Particle Swarm Optimisation (PSO), Grey Wolf Optimiser (GWO), and an enhanced GWO algorithm(Zakian et al., 2021). The Industrial Revolution marked a turning point in engineering history, as advancements in mathematics and physics gave rise to disciplines such as civil and mechanical engineering(HOFFECKER, 2005). Post-Industrial Revolution, the growing

demand for rapid construction and increased resource consumption led to challenges such as economic constraints, unsustainable use of non-renewable resources, excessive hazardous waste, and greenhouse gas emissions. These issues not only impact the environment but also jeopardise future generations(HOFFECKER, 2005). In response, advances in science and technology have led to the development of metaheuristic algorithms, which have become essential engineering tools for optimising large-scale, complex problems due to their problem-solving capabilities (Kaveh, 2017).

These algorithms combine stochastic methods with search strategies to identify optimal solutions for diverse problems. Nature-inspired metaheuristic algorithms have gained significant popularity in engineering applications in recent years and are classified into four main categories: evolutionary-based, physics-based, swarm-based, and human behaviour-based. Despite their diverse inspirations, they all share two fundamental components: exploration and exploitation(Mirjalili & Lewis, 2016). Exploration refers to the algorithm's ability to conduct a global search of the solution space, offering advantages such as avoiding local optima and increasing the likelihood of finding global optima. However, it may also lead to slower convergence rates and higher computational resource consumption(Talbi, 2009). Previous years have seen numerous studies on conventional frame structure optimisation, with various metaheuristic algorithms being developed. The Genetic Algorithm has been employed by researchers such as Rajeev and Krishnamoorthy(Rajeev & Krishnamoorthy, 1992), Pezeshk et al(Pezeshk et al., 2000), and Kaveh and Rahami(Kaveh & Rahami, 2006)for steel frame optimisation problems. Other metaheuristic algorithms including improved Ant Colony Optimisation(Kaveh & Talatahari, 2010a), Imperialist Competitive Algorithm(Kaveh & Talatahari, 2010b), Big Bang-Big Crunch(HasançEbi, & Kazemzadeh Azad, 2012), Bat Algorithm(Hasançebi & Carbas, 2014), and Artificial Bee Colony(Aydoğdu et al., 2016) have been investigated by various scholars. TalaTaheri et al.(Talatahari et al., 2015) proposed a hybrid Eagle Strategy with Differential Evolution, implemented through SAP2000 and MATLAB interfaces for optimal structural frame design. Khajeh et al.(Khajeh et al., 2017) developed a hybrid method combining Particle Swarm Optimisation with Grid Search to reduce computational time. Mirjalili et al. introduced the Grey Wolf Optimiser in 2014(Mirjalili et al., 2014) and the Whale Optimisation Algorithm in 2016(Mirjalili & Lewis, 2016).

In this paper, the grey wolf optimisation and whale optimisation methods have been developed for weight optimisation of steel pipe rack structures while complying with the seismic design code for oil industry facilities and structures(Seismology, International Institute of Earthquake Engineering and structures Edition 4, 2023) and design constraints. This research presents a method for designing steel pipe racks through the connection of computational software MATLAB and ETABS2016, which enables the use of optimisation algorithms. The connection between these two software programs is established through the ETABS API. The connection process operates as follows: MATLAB sends the required information such as geometric specifications and analysis settings to ETABS through API functions. Subsequently, ETABS conducts the analysis and design and returns the desired results such as stresses and displacements to MATLAB. MATLAB uses this data to execute the optimisation algorithm and optimises the structural sections. This process is repeated until an optimal design is achieved. In this method, the pipe rack structure is modelled in ETABS2016 in full compliance with the seismic design code for

oil industry facilities and structures and AISC-LRFD(AISC, 2010), after which the optimisation process is carried out. The Auto Select List feature in ETABS is designed to select optimal sections based on load-to-capacity ratios. This method typically does not consider important structural constraints such as drift limitations in the section selection process. Consequently, sections selected solely based on strength criteria may exhibit undesirable structural drift and violate code limits. In the present research, in addition to observing member strength requirements, drift control has also been incorporated into the design process. This approach ensures that the obtained results are not only theoretically reliable but also directly applicable to the design of pipe rack structures.

2. Design of Pipe Rack Structures

In a large portion of petrochemical facilities, pipe rack structures are used. As shown in (Figure 1), these structures are designed as open frameworks to facilitate the passage and placement of components such as pipes, mechanical and electrical equipment, and due to their application in transporting fluids and petroleum condensates, they are constructed on a large scale.

Figure 1. Steel Pipe-Rack

Among the characteristics of pipe racks are geometric irregularities in height and length, as well as multiple dead and live loads from the equipment and pipes supported by these structures, along with seismic and thermal loads. This results in complex geometries for this type of industrial structure, making the process of achieving an optimal design challenging(Hsu & Jean, 2003). In the design of these structures, moment frames are used in one direction to provide access to operational equipment and installation of main pipes. Moment frames, while providing accessibility for equipment and pipe installation, can be vulnerable to excessive lateral deformations under seismic loads. In the other direction of the structure, braced frames are typically used due to less need for access to equipment installed on the pipe rack. These frames provide an efficient structural system for delivering stiffness and can reduce their ductility against lateral loads(Hsu & Jean, 2003).

Structural design begins with defining the applied loads. These loads include dead loads, live loads, wind loads, seismic loads, and other operational loads that are determined based on the type of structure and its application. The loading process ensures that all influencing factors are considered in the design. After defining the loads, structural modelling is completed in ETABS2016. This software uses the finite element method to analyse the structure's behaviour under the defined loads. The outputs of this analysis include stresses, displacements, and internal member forces that form the basis for design. The design of structural members is performed according to the relevant codes to ensure the structure can withstand the applied loads and safety criteria are met. It is essential to note that in the design process, the main objective is not only to ensure structural safety and performance but also to consider its economic optimisation. In the design of pipe rack structures, various loads including dead, live, operational, and seismic loads are applied, with explanations for each provided in (Table 1) (M. DRAKE & J. WALTER, 2010; Shahiditabat & Mirghaderi, 2013).

Table 1. Applied Loads on Pipe Rack Structure

Load Type	Symbol	Description
Dead Load	D	Self-weight of structure and permanent equipment (access platforms, fire-fighting equipment) supported by the structure.
Thermal Load	T	Includes environmental thermal effects.
Structural Seismic Load	EQx, EQy	Seismic forces generated by the structure itself.
Large-Diameter Pipe Seismic Load	EQx-P, EQy-P	Seismic forces from large-diameter pipes, calculated by piping engineers.
Empty Pipe Load	EMP, EMP-Frx, EMP-Fry	Load caused by the weight of empty pipes.
Operating Pipe Load	OP, OP-Frx, OP-Fry	Load from pipe weight, fluid acceleration, and thermal effects of internal fluid.
Fabrication Imperfection Load	Notional	Accounts for potential member out-of-plumb condition and initial imperfections.
Wind Load	Wind	Loads resulting from wind pressure.
Hydrotest Load	HYD	Load generated by pipe weight and water mass during pipeline testing.

The main loads acting on the structure include operational loads, seismic loads, and thermal loads. Pipes with diameters greater than 12 inches are considered large-diameter pipes. After determining the pipe routing path and calculating the forces exerted on the structure by the pipes, along with performing the related calculations, the pipe rack loading diagrams (SLD[1]) are prepared. Based on these diagrams, the design engineer carries out the design process and determines the section sizes.

3. Pipe Rack Design Criteria

The objective of structural optimisation is to reduce member sizes while considering applied loads to decrease weight and required construction materials, thereby reducing overall costs(Togˇan, 2012).

In most structural optimisation studies, the objective function is defined as Eq. (1):

$$f(x) = \sum_{i=1}^{n} (\gamma l A)_i \tag{1}$$

In Eq. (1), l represents element length, A denotes member cross-sectional area, γ is the specific weight of steel, $f(x)$ is the objective function, n indicates the number of members, and i represents the current frame member(Mahallati et al., 2018).

The AISC-LRFD code(AISC, 2010) has been employed for the design and capacity verification of structural members. The optimisation constraints for frame design include: (1) the member capacity constraint (V_i^{σ}), and (2) the inter-storey drift constraint as defined in Eq. (2) and (3).

$$V_i^{\sigma} = \left|\frac{\sigma_i}{\sigma_{\alpha}^{i}}\right| - 1 \leq 0 \qquad i = 1,2,\ldots n \tag{2}$$

$$\frac{\delta_{max}}{\bar{\delta}} - 1 \leq 0 \tag{3}$$

1. Structure Loading Diagram or Single Load Diagram

In Eq. (2) and (3), σi is the internal force in member i, $\sigma_{\alpha}^{\ i}$ is the load-bearing capacity of member i, δ_{max} is the relative displacement of each storey level, and $\bar{\delta}$ is the allowable relative displacement.

The design constraints (v_i^I) for frame members according to AISC-LRFD(AISC, 2010)are based on Eq. (4), (5) and (6):

$$v_i^I = \frac{P_u}{2\emptyset_c p_n} + \left(\frac{M_{ux}}{\emptyset_b M_{nx}} + \frac{M_{uy}}{\emptyset_b M_{ny}}\right) \ldots \leq 1 \quad \text{for } \frac{P_u}{\emptyset_c p_n} < 0.2 \quad (4)$$

$$v_i^I = \frac{P_u}{\emptyset_c p_n} + \frac{8}{9}\left(\frac{M_{ux}}{\emptyset_b M_{nx}} + \frac{M_{uy}}{\emptyset_b M_{ny}}\right) \ldots \leq 1 \quad \text{for } \frac{P_u}{\emptyset_c p_n} \geq 0.2 \quad (5)$$

In Eq. (4) and (5), φ_b is the resistance reduction factor for bending with a value of 0.9, φ_c is the resistance reduction factor in compression equal to 0.9 and in tension equal to 0.85, P_u is the existing compressive force, P_n is the nominal tensile or compressive resistance, M_{uy} is the existing (amplified) bending moment about the y-axis (weak axis), M_{ny} is the nominal bending resistance about the y-axis (weak axis), M_{ux} is the existing (amplified) bending moment about the x-axis (strong axis), and M_{nx} is the nominal bending resistance about the x-axis (strong axis).

For shear capacity, Eq. (6) has been applied as a constraint:

$$\frac{V_u}{\varphi_v V_n} \leq 1 \quad (6)$$

In Eq. (6), V_u is the existing shear force and V_n is the nominal shear resistance of each member, and φ_v is the shear resistance reduction factor equal to 1.

The stability of frame members has been verified according to Eq. (7) and (8):

$$\gamma_m = \frac{Kl_m}{r_m} \leq 200 \quad \textit{For Compressive Members} \quad (7)$$

$$\gamma_m = \frac{l_m}{r_m} \leq 300 \quad \textit{For Tensile Member} \quad (8)$$

In Eq. (7) and (8), l_m is the unbraced length of the member, r_m is the radius of gyration of the member, and K is the effective length factor. Frame structures are controlled by displacement limits, which are determined according to the seismic design code for oil industry facilities and structures.

For calculating compressive and Euler stresses, the effective length factor (K) is required. The value of K for beams is equal to one, and for columns it is obtained from Eq. (9).

$$K = \sqrt{\frac{1.6G_AG_B + 4G_AG_B + 7.5}{G_A + G_B + 7.5}} \geq 1 \quad (9)$$

The value of K for braces is calculated from Eq. (10):

$$K = \frac{3G_AG_B + 1.4(G_A + G_B) + 0.64}{3G_AG_B + 2(G_A + G_B) + 1.28} \quad (10)$$

In Eq. (9) and (10), G_A and G_B represent the boundary conditions at both ends of the compressive member(Salama, 2013).

4. Grey Wolf Optimisation Algorithm

The general form of the optimisation problem is shown in Eq. (11).

$$\textit{Minimize } f(x)$$

$$\textit{Subject to: } \begin{cases} h_i(x) = 0 & i = 1, 2 \ldots, m_1 \\ g_j(x) < 0 & j = 1, 2 \ldots, m_2 \\ L_n < x_n < U_n & n = 1, 2 \ldots, m_3 \end{cases} \quad (11)$$

In Eq. (11), x represents an n-dimensional vector that denotes the design variables. g and h represent inequality and equality constraints, respectively. L and U indicate the lower and upper bounds of the design variables. m_1, m_2, and m_3 specify the number of equality constraints, inequality constraints, and the dimensions of the search space, respectively. The space where all constraints are satisfied is called the decision space, which determines the number of decision variables(Mahallati et al., 2018).

The Grey Wolf Optimiser (GWO) algorithm was introduced by Mirjalili et al. in 2014. This metaheuristic algorithm is inspired by the hunting behaviour of grey wolves and belongs to the category of swarm intelligence and population-based algorithms(Mirjalili et al., 2014).

The algorithm is developed and mathematically modelled based on the social hierarchy and cooperative hunting behaviour of grey wolves. Grey wolves are known as apex predators at the top of the food chain.

They typically live in packs averaging 5-12 wolves. A distinctive characteristic of grey wolves is their strict social hierarchy. The pack leader, which can be male or female, is called the alpha wolf; this wolf is not necessarily the strongest in the pack but is the best in terms of pack management. The alpha wolf is primarily responsible for making important decisions regarding hunting, sleeping locations, and wake-up times, and other wolves must follow its orders(Mech, 1999).

The second level in the hierarchy consists of beta wolves, which serve as advisors to the alpha. These wolves follow the alpha's commands, reinforce its decisions, and also give orders to other wolves. The lowest ranking wolves are called omega wolves. These wolves help maintain the pack structure and are the last to eat. Wolves that don't belong to any of the above three categories are called delta wolves. These wolves follow the commands of alphas and betas but give orders to omega wolves. Delta wolves warn the pack when they sense danger and help ensure the pack's safety. Elderly and caretaker wolves belong to this group(Mirjalili et al., 2014).

In the GWO algorithm, the prey represents the best-known solution at the current moment, which the search agents follow to improve their positions. The hunting process represents finding the best possible solution to the problem. To model the social hierarchy in the GWO algorithm, the best position or solution is called alpha, the second-best solution is called beta, the third-best solution is called delta, and other solutions are called omega. For modelling the encircling behaviour of prey, Eq. (12) to (15) have been proposed:

$$\vec{X}(\mathrm{t}+1) = \overrightarrow{X_p}(t) - \vec{A}.\vec{D} \tag{12}$$

$$\vec{D}(t) = \left|\vec{C}.\overrightarrow{X_p}(t) - \vec{X}(t)\right| \tag{13}$$

$$\vec{A} = \vec{a}(2.\overrightarrow{r_1} - 1) \tag{14}$$

$$\vec{C} = 2.\overrightarrow{r_2} \tag{15}$$

In Eq. (12) to (15), $\vec{X}(t)$ represents the position of the grey wolf at iteration t, $\overrightarrow{X_p}(t)$ represents the position of the prey (the best known solution at that moment) at iteration t, and $\vec{D}(t)$ represents the distance between the grey wolf's position and the prey's position at iteration t. The component $\vec{a}$ decreases linearly from 2 to zero, while r_1 and r_2 are random numbers between zero and one. The grey wolf algorithm has two parameters, $\vec{C}$ and $\vec{A}$, which control the exploration and exploitation processes. During the search for the optimal solution, the actual position of the hunt is unknown. Therefore, the best position obtained up to that point is considered as the hypothetical position of the prey, which is typically the position of the alpha wolf representing the current best solution. The second and third best solutions, belonging to the beta and delta wolves respectively, are also considered as potential prey positions. Thus, the three best solutions found are stored, and other search agents (omega wolves) are required to update their positions according to the positions of alpha, beta, and delta. Eq. (16) to (19) represent these relationships:

$$\overrightarrow{X_1}(t) = \overrightarrow{X_\alpha}(t) - \overrightarrow{A_1}.\overrightarrow{D_\alpha}(t) \quad \& \quad \overrightarrow{D_\alpha}(t) = \left|\overrightarrow{C_1}.\overrightarrow{X_\alpha}(t) - \vec{X}(t)\right| \tag{16}$$

$$\overrightarrow{X_2}(t) = \overrightarrow{X_\beta}(t) - \overrightarrow{A_2}.\overrightarrow{D_\beta}(t) \quad \& \quad \overrightarrow{D_\beta}(t) = \left|\overrightarrow{C_2}.\overrightarrow{X_\beta}(t) - \vec{X}(t)\right| \tag{17}$$

$$\overrightarrow{X_3}(t) = \overrightarrow{X_\delta}(t) - \overrightarrow{A_3}.\overrightarrow{D_\delta}(t) \quad \& \quad \overrightarrow{D_\delta}(t) = \left|\overrightarrow{C_3}.\overrightarrow{X_\delta}(t) - \vec{X}(t)\right| \tag{18}$$

$$\vec{X}(\mathrm{t}+1) = \frac{\overrightarrow{X_1}(t) + \overrightarrow{X_2}(t) + \overrightarrow{X_3}(t)\big)}{3} \tag{19}$$

Optimisation involves two opposing processes: exploration and exploitation(Črepinšek et al., 2013). The exploration process aims to discover new areas of the search space by introducing sudden changes in solutions, preventing potential solutions from becoming trapped in local optima. The exploitation process works to improve existing solutions by examining their neighbourhoods more thoroughly and applying gradual changes to reach the optimal solution. Since exploration and exploitation are opposing processes, the algorithm must maintain a balance between them. The parameter C generates random values in the interval [0,2], influencing the prey's next position. When C >1, the algorithm moves to explore new areas, attempting to move away from the current position to potentially find better solutions and avoid local optima. In this case, the exploration process becomes more prominent than exploitation. When $\vec{C}$ becomes greater than one, according to Eq. (13), $\vec{D}$ generally increases, meaning the wolves' position changes occur over a larger range, expanding the search space. Conversely, when $\vec{C}$ is less than one, the focus shifts more toward exploiting existing areas. The other variable is parameter $\vec{A}$, which is defined based on the value of $\vec{a}$ in Eq. (20), decreasing linearly from 2 to 0:

$$\vec{a} = 2 - \mathrm{t}\left(\frac{2}{\mathrm{T}}\right) \tag{20}$$

When $\vec{A}$ is greater than 1 or less than -1, the value of $\vec{A}.\vec{D}$ increases, resulting in larger changes in the wolves' new positions. This means the search range and movement toward unknown and new areas increase, making the exploration process more prominent. On the other hand, when $\vec{A}$ falls within the interval [-1,1], the changes in new positions are smaller, aiding the exploitation process by allowing the algorithm to focus more on areas close to its current position(Mirjalili et al., 2014).

The pseudocode of the Grey Wolf Optimisation algorithm is presented in (Figure 2).

Initialize the grey wolf population X_i (i = 1, 2, ..., n)
Initialize a, A, and C
Calculate the fitness of each search agent
X_α=the best search agent
X_β=the second best search agent
X_δ=the third best search agent
while *(t < Max number of iterations)*
  for *each search agent*
    Update the position of the current search agent by equation (19)
  end for
  Update a, A, and C
  Calculate the fitness of all search agents
  Update X_α, X_β, and X_δ
  t=t+1
end while
return X_α

Figure 2. Pseudocode of the Grey Wolf Optimisation Algorithm(Mirjalili et al., 2014)

5. Whale Optimisation Algorithm

The Whale Optimisation Algorithm (WOA) is inspired by the hunting behaviour of a specific species of whales and was introduced by Mirjalili and Lewis in 2016(Mirjalili & Lewis, 2016). Whales are the largest mammals on Earth. Among the seven main species, we can mention killer whales, minke whales, sei whales, humpback whales, right whales, fin whales, and blue whales. These mammals possess unique characteristics including thinking ability, judgment, communication skills, and emotional capacity. A notable species is the humpback whale, which employs a distinctive hunting method called bubble-net feeding. In this method, whales create bubbles in a spiral path to trap their prey. It should be noted that this hunting technique is unique to humpback whales. The mathematical

modelling of this behaviour is explained below(Mirjalili & Lewis, 2016).

5.1. Encircling Prey

In the optimisation process, as mentioned in Section 4, the prey represents the best-known solution at the current moment, which the whales (search agents) follow to improve their positions, while the hunt represents the best possible solution to the problem that the algorithm seeks to find. Humpback whales identify the prey's location and encircle it. Since the exact location of the optimal solution is unknown, the algorithm assumes that the current best solution is close to the optimal point. Other search agents update their positions to move closer to the best solution. Eq. (21) and (22) represent this behaviour.

$$\vec{D} = \left|\vec{C}.\overrightarrow{X^*}(t) - \vec{X}(t)\right| \quad (21)$$

$$\vec{X}(t+1) = \overrightarrow{X^*}(t) - \vec{A}.\vec{D} \quad (22)$$

In Eq. (21) and (22), $\vec{A}$ and $\vec{D}$ are coefficients that change dynamically, and t represents the iteration number. $\overrightarrow{X^*}(t)$ denotes the current best solution found, while $\vec{X}$ represents the position of the search agent. The vectors $\vec{A}$ and $\vec{C}$ are defined in Eq. (23) and (24).

$$\vec{A} = 2\vec{a}.\vec{r} - \vec{a} \quad (23)$$

$$\vec{C} = 2.\vec{r} \quad (24)$$

The component $\vec{a}$ decreases linearly from 2 to 0, and r represents a random vector between 0 and 1. The combination of Eq. (21) to (24) helps the algorithm simulate the prey encirclement process.

5.2. Position Update with Spiral Motion

In this method, first the distance between the whale's position and the prey is calculated, and then Eq. (25) is used to simulate the whale's spiral movement toward the prey.

$$\vec{X}(t+1) = \overrightarrow{D'}.e^{bl}.\cos(2\pi l) + \overrightarrow{X^*}(t) \quad (25)$$

The value D' is obtained from Eq. (26).

$$\overrightarrow{D'} = \left|\overrightarrow{X^*}(t) - \vec{X}(t)\right| \quad (26)$$

In Eq. (25), b is a constant value that determines the shape of the spiral movement, and l is a random number in the interval [-1,1]. Humpback whales move in a gradually shrinking circular path that forms a spiral around their prey. To model this dual behaviour, the algorithm is assumed to select either the shrinking encircling method or the spiral model with a 50% probability to update the whales' positions. The mathematical model of this process is shown in Eq. (27) and (28) (Mirjalili & Lewis, 2016).

$$\vec{X}(t+1) = \overrightarrow{X^*}(t) - \vec{A}.\vec{D} \quad for\ p < 0.5 \quad (27)$$

$$\vec{X}(t+1) = \overrightarrow{D'}.e^{bl}.cos(2\pi l) \ldots + \overrightarrow{X^*}(t) \quad for\ p \geq 0.5 \quad (28)$$

Where p is a random number in the interval [0,1].

5.3. Exploration Phase

In the exploration phase, changes in the vector $\vec{A}$ are used. Whales search for prey randomly based on each other's positions. To ensure effective exploration of the search space, the value of $\vec{A}$ must be greater than 1 or less than -1. During this phase, whale positions are updated based on a randomly selected search agent, which is exactly opposite to the exploitation phase where the best-known solution is used for position updates. This approach, when $|\vec{A}|>1$, focusses on the exploration process, allowing the algorithm to search more extensively throughout the solution space for the optimal answer. The mathematical model of this process is shown in Eq. (29) and (30).

$$\vec{D} = \left|\vec{C}.\overrightarrow{X_{rand}} - \vec{X}(t)\right| \quad (29)$$

$$\vec{X}(t+1) = \overrightarrow{X_{rand}} - \vec{A}.\vec{D} \quad (30)$$

The whale algorithm begins with a random set of solutions. In each iteration, search agents update their positions either based on a random operation or the best solution found so far. Parameter a gradually decreases from 2 to 0 to enable both exploration and exploitation. When $|\vec{A}|>1$, a random search operation is selected, while when $|\vec{A}|<1$, the best solution is used to update whale positions. Depending on the value of p, the algorithm can switch between circular or spiral movement patterns(Mirjalili & Lewis, 2016). Throughout the algorithm's execution, the prey position is continuously updated as whales attempt to reach the optimal solution. This process continues until the algorithm converges and extracts the optimal solution.

The pseudocode of the Whale Optimisation Algorithm is shown in (Figure 3).

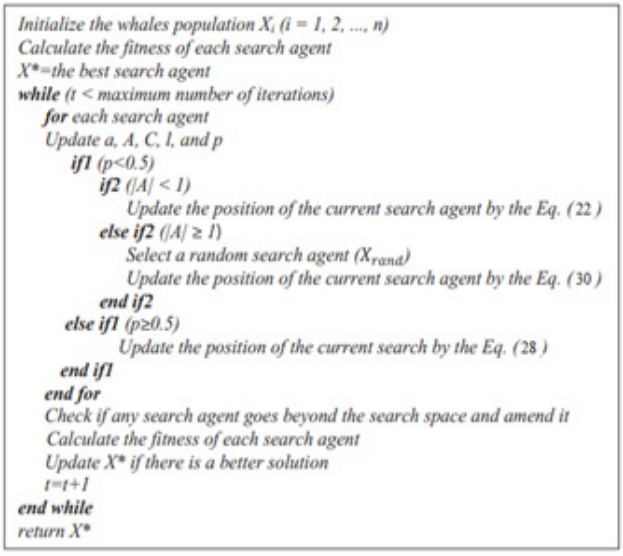

Figure 3. Pseudocode of the Whale Optimisation Algorithm(Mirjalili & Lewis, 2016)

6. Constraint Handling

In constrained optimisation problems, adhering to problem constraints is of utmost importance. In the studied optimisation algorithms, the penalty method is employed to guide solutions toward the feasible region. In this method, if a solution violates any constraints, its objective function value is modified by adding a penalty term. This penalty term is calculated as the product of a penalty coefficient and the degree of constraint violation.

7. Numerical Examples

Two steel pipe rack examples are presented to evaluate the performance of grey wolf and whale optimisation algorithms for this type of structure. The modelling was performed using the seismic design code for oil industry facilities and structures(Seismology, International Institute of Earthquake Engineering and structures Edition 4, 2023) along with AISC-LRFD(AISC, 2010) provisions. The structures feature ordinary concentric braced frames in the longitudinal direction and intermediate moment frames in the transverse direction. Due to the absence of rigid floor diaphragms, horizontal bracing is employed to enhance seismic performance and structural integrity.

For these structures, the steel density equals 7850 kg/m^3 with an elastic modulus of 200 GPa. The steel has a yield stress of 240 MPa and ultimate stress of 370 MPa. As standard practice for seismic calculations, equivalent static analysis and response spectrum analysis based on design codes are performed for structural evaluation and design. This analysis aims to determine seismic forces acting on the structure and verify design compliance with code requirements.

The design wind speed of 125 km/h (hourly average) has been applied to the structure according to ASCE7-10 code(Engineers American Society of Civil, 2010).

The lateral displacement of pipe rack structures is calculated using Eq. (31) based on the seismic design code for oil industry facilities and structures(Seismology, International Institute of Earthquake Engineering and structures Edition 4, 2023).

$$\delta_{DE} = \frac{C_d \times \delta_e}{I} \tag{31}$$

In Eq. (31), C_d represents the displacement amplification factor (4 for intermediate moment frames and 3.25 for ordinary concentric braced frames), δ_e denotes the elastic lateral displacement at each level due to lateral loads, I is the importance factor (1.25), and δ_{DE} indicates the design (inelastic) lateral displacement.

According to the relevant code, the allowable inter-storey drift ratio for pipe rack structures is considered as 0.01 of the storey height(Seismology, International Institute of Earthquake Engineering and structures Edition 4, 2023). P-Δ effects have been included, and load combinations follow AISC-LRFD(AISC, 2010) provisions.

The structural finite element model analysis is performed using ETABS2016, after which the optimisation algorithm coded in MATLAB environment gradually updates the design parameters. In this study, a termination criterion based on the number of iterations was employed to conclude the execution of the algorithm. This means that the algorithm automatically stops after completing a predefined number of iterations. This method was chosen due to its simplicity and high efficiency.

7.1. Steel Pipe Rack Example 1

The first example (Figure 4) shows a three-storey steel pipe rack with 99 members. The studied structure has three main spans in the longitudinal direction (x) with a length of 5 metres and one main span in the transverse direction (y) with a length of 6 metres, located at three elevation levels (z) with height codes of 4, 7, and 9.5 metres above ground level. Due to the absence of a roof and rigid diaphragm, horizontal bracing is used for better and more integrated performance against earthquakes. (Figure 4) provides an overall view of the structure.

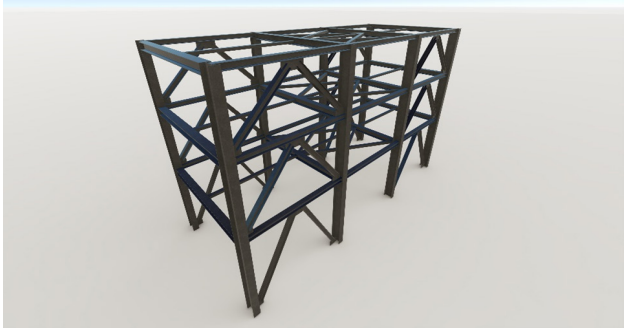

Figure 4. Steel Pipe-Rack Example 1

(Table 2) shows the seismic coefficient applied to the structure.

Table 2. Earthquake Coefficients Applied to the Structure of Steel Pipe-Rack Example 1

Type of Applied Load	Direction of Load Application	Value of Coefficient C	Value of Coefficient K
Earthquake	Direction X	0.461	1
	Direction Y	0.393	1

The number of analyses for the grey wolf and whale optimisation algorithms has been set to 7,500. The population size is set to 150, and the number of algorithm iterations is set to 50.

(Figure 5) and (Table 3) show the grouping of pipe rack sections and their corresponding colours. The structural members are categorised into 10 groups:

Table 3. Grouping and Number of Sections in Steel Pipe-Rack Example 1

Groups										
Section Type	Column				Beam			Lateral Brace		Floor bracing
Group Number	1	2	3	4	5	6	7	8	9	10
Number of Elements in Each Group	8	8	8	4	8	6	12	8	16	21
Colour										

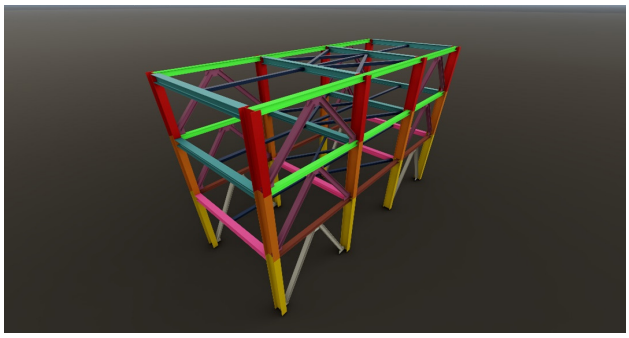

Figure 5. Display of Section Grouping in Steel Pipe-Rack Example 1

HEA and HEB sections are used for columns, beams, and lateral bracing, while box sections are used for floor bracing according to (Tables 4 and 5).

Table 4. HE Sections Used in Steel Pipe-Rack Example 1

HE100A	HE100B	HE120A	HE140A	HE160A	HE180A	HE200A
HE200B	HE220A	HE220B	HE240A	HE240B	HE260A	HE260B
HE280A	HE280B	HE300A	HE300B	HE320A	HE320B	HE340A
HE340B	HE360A	HE360B	HE400A	HE400B	HE450A	HE450B
HE500A	HE500B	HE550B	HE600B	HE650B	HE700B	

Table 5. BOX Sections Used in Steel Pipe-Rack Example 1

BOX140×70×3.6	BOX140×70×4	BOX140×70×4.5	BOX140×70×5	BOX140×70×5.4
BOX140×70×5.9	BOX140×70×7.1	BOX140×70×8	BOX140×70×10	BOX140×70×12.5
BOX140×98×5	BOX140×98×5.4	BOX140×98×5.9	BOX140×98×7.1	BOX140×98×8
BOX140×98×10	BOX140×98×12.5	BOX140×98×14.2	BOX140×98×16	BOX140×98×17.5

Thus, the 99 elements are divided into 10 groups, with groups 1 to 9 including 34 sections and group 10 including 20 sections for selection, creating a complex optimisation problem.

(Table 6) and (Figure 6) show the results obtained from the grey wolf and whale optimisation algorithms for the discussed pipe rack.

Table 6. Comparison of Results for the Whale and Grey Wolf Algorithms in Steel Pipe-Rack Example 1

Group Number of Member	GWO	WOA
1	HE450A	HE450A
2	HE450A	HE450A
3	HE360A	HE280A
4	HE450A	HE400A
5	HE320A	HE360A
6	HE220A	HE220A
7	HE180A	HE160A
8	HE200A	HE180A
9	HE140A	HE140A
10	TUBO140X98X5.4	TUBO140X98X5
Weight (KN)	264.79	264.1
Number of Analyses	7500	7500

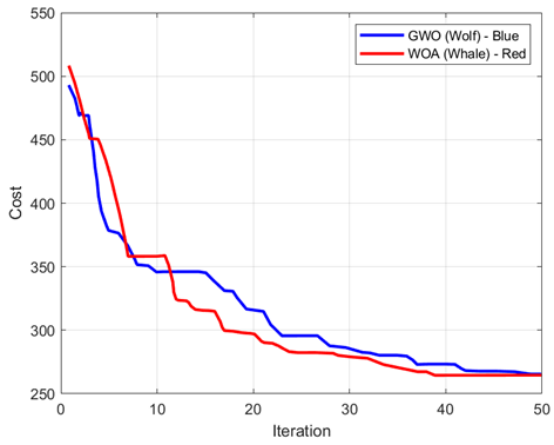

Figure 6. Optimisation Process in Steel Pipe Rack Example 1 Using the Grey Wolf and Whale Optimisation Algorithms

7.2. Steel Pipe Rack Example 2

The second example examines a two-storey steel pipe rack structure consisting of 138 members. The structure under investigation contains four main spans measuring 5 metres in the longitudinal (x) direction and two main spans of 6 metres in the transverse (y) direction. The structure is positioned at two elevation levels: 6.85 metres and 8.35 metres above ground level. (Figure 7) provides an overall illustration of the structure. (Table 7) presents the seismic coefficients applied to the structure.

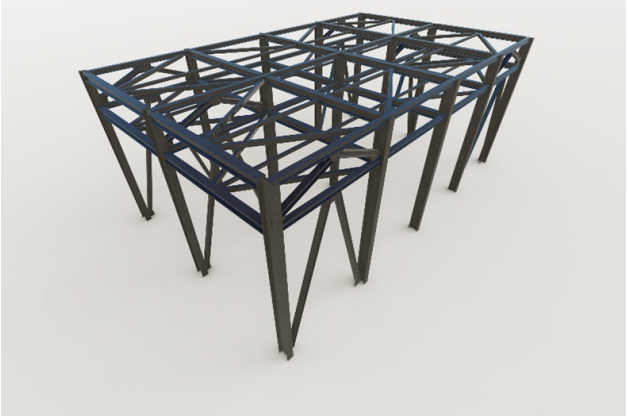

Figure 7. Steel Pipe-Rack Example 2

Table 7. Earthquake Coefficients Applied to the Structure of Steel Pipe-Rack Example 2

Type of Applied Load	Direction of Load Application	Value of Coefficient C	Value of Coefficient K
Earthquake	Direction X	0.461	1
	Direction Y	0.428	1

The whale optimisation algorithm was configured to perform 7,500 analyses. The population size is set to 150, and the number of algorithm iterations is set to 50.

(Figure 8) and (Table 8) display the pipe rack section groupings and their corresponding colour coding. The structural members are categorised into nine groups:

Table 8. Grouping and Number of Sections in Steel Pipe-Rack Example 2

Groups									
Section Type	Column	Beam				Lateral Brace		Floor bracing	
Group Number	1	2	3	4	5	6	7	8	9
Number of Elements in Each Group	30	10	10	12	12	12	12	20	20
Colour									

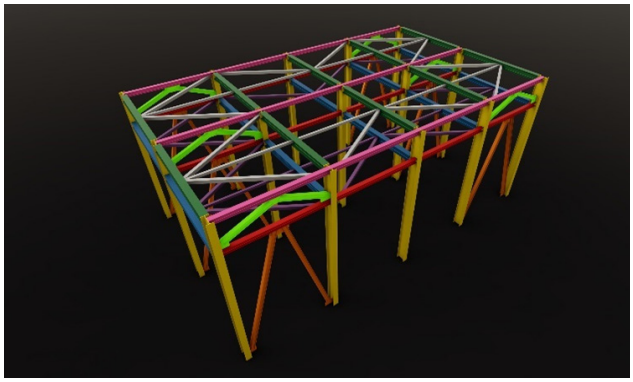

Fig. 8. Display of Section Grouping in Steel Pipe-Rack Example 2

columns, beams, and lateral bracing utilise HEA and HEB sections, while floor bracing employs box sections as detailed in (Tables 9 and 10).

Table 9. HE Sections Used in Steel Pipe-Rack Example 2

HE100A	HE100B	HE120A	HE140A	HE160A	HE180A	HE200A
HE200B	HE220A	HE220B	HE240A	HE240B	HE260A	HE260B
HE280A	HE280B	HE300A	HE300B	HE320A	HE320B	HE340A
HE340B	HE360A	HE360B	HE400A	HE400B	HE450A	HE450B
HE500A	HE500B	HE550B	HE600B	HE650B	HE700B	

Table 10. BOX Sections Used in Steel Pipe-Rack Example 2

BOX140×98×5	BOX140×98×5.4	BOX140×98×5.9	BOX140×98×7.1	BOX140×98×8
BOX140×98×10	BOX140×98×12.5	BOX140×98×14.2	BOX140×98×16	BOX140×98×17.5
BOX140×140×7.1	BOX140×140×8	BOX140×140×10	BOX140×140×12.5	BOX140×140×14.2
BOX140×140×16	BOX140×140×17.5	BOX140×140×20	BOX140×140×22.2	BOX140×140×25

Consequently, the 138 elements are divided into nine groups, with groups 1 through 7 offering 34 section options each, and groups 8 and 9 providing 20 section options each, creating a complex optimisation challenge.

(Table 11) and (Figure 9) present the results obtained from applying the grey wolf and whale optimisation algorithms to the pipe rack under consideration.

Table 11. Comparison of Results for the Whale and Grey Wolf Algorithms in Steel Pipe-Rack Example 2

Group Number of Member	GWO	WOA
1	HE450B	HE450B
2	HE400A	HE400A
3	HE450A	HE400A
4	HE280A	HE280A
5	HE180A	HE180A
6	HE260A	HE260A
7	HE180A	HE100A
8	TUBO140X140X7.1	BOX140×140×7.1
9	TUBO140X140X7.1	BOX140×140×7.1
Weight (KN)	565.907	550.65
Number of Analyses	7500	7500

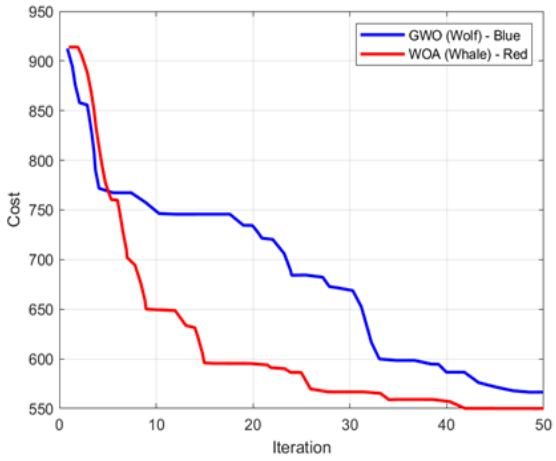

Figure 9. Optimisation Process in Steel Pipe-Rack Example 2 Using the Grey Wolf and Whale Optimisation Algorithms

8. Conclusions

In this research, the grey wolf and whale metaheuristic algorithms were used to optimise steel pipe rack structures. The performance of these methods was evaluated on two steel pipe racks. Establishing a connection between MATLAB and ETABS2016 enabled automated management of design inputs and outputs, which led to weight reduction of structures while complying with code requirements. The results show that both algorithms have high capability in optimising this type of steel structure. Using these methods in industrial structure design, especially in oil and gas projects, can help reduce costs and increase productivity. Furthermore, the high optimisation capability of the studied algorithms makes them applicable to other industrial structures as well. Finally, this research shows that the mentioned methods can be effective and practical tools for structural engineers and, by optimising pipe racks, can play an important role in reducing costs of civil engineering projects. For future research, it is recommended to explore the use of alternative optimisation algorithms with faster convergence rates. Additionally, the optimisation of concrete pipe-rack structures could be investigated.

References

Agency International Energy. (2024). World Energy Outlook 2024. International Energy Agency.

AISC. (2010). Specifications for structural steel buildings. IL: AISC.

Aydoğdu, i, Akın, A., & Saka, M. P. (2016). Design optimization of real world steel space frames using artificial bee colony algorithm with Levy flight distribution. Advances in Engineering Software, 92, 1-14. https://doi.org/10.1016/j.advengsoft.2015.10.013.

Črepinšek, M., Liu, S., & Mernik, M. (2013). Exploration and Exploitation in Evolutionary Algorithms: A Survey. ACM Computing Surveys, 45(3). https://doi.org/10.1145/2480741.2480752.

Engineers American Society of Civil. (2010). Minimum Design Loads for Buildings and Other Structures (ASCE/SEI 7-10). American Society of Civil Engineers.

Hasançebi, O., & Carbas, S. (2014). Bat inspired algorithm for discrete size optimization of steel frames. Advances in Engineering Software, 67, 173-185. https://doi.org/10.1016/j.advengsoft.2013.10.003.

HasançEbi, O., & Kazemzadeh Azad, S. (2012). An exponential big bang-big crunch algorithm for discrete design optimization of steel frames. Computers and Structures, 110-111, 167-179. https://doi.org/10.1016/j.compstruc.2012.07.014.

HOFFECKER, J. F. (2005). Innovation and Technological Knowledge in the Upper Paleolithic of Northern Eurasia. Evolutionary Anthropology, 14, 186-198. https://doi.org/10.1002/evan.20066.

Hsu, H. L., & Jean, S. Y. (2003). Improving seismic design efficiency of petrochemical facilities. Practice Periodical on Structural Design and Construction, 8(2), 107-117. https://doi.org/10.1061/(ASCE)1084-0680(2003)8:2(107).

J Singh, N., & Ishtiyaque, M. (2016). Optimized Design & Analysis of Steel Pipe Racks for Oil

& Gas Industries as per International Codes & Standards. International Journal of Research in Engineering and Technology, 5(10).

Karimi, M., Hosseinzadeh, N., Hosseini, F., & Kazem, N. (2011). Seismic Evaluation of Pipe Rack Supporting Structures in a Petrochemical Complex in Iran. International Journal of Advanced Structural Engineering, 3(1), 111-120.

Kaveh, A., & Rahami, H. (2006). Nonlinear analysis and optimal design of structures via force method and genetic algorithm. Computers & Structures, 84(12), 770-778. https://doi.org/10.1016/j.compstruc.2006.02.004.

Kaveh, A., & Talatahari, S. (2010a). An improved ant colony optimization for the design of planar steel frames. Engineering Structures, 32(3), 864-873. https://doi.org/10.1016/j.engstruct.2009.12.012

Kaveh, A., & Talatahari, S. (2010b). Optimum design of skeletal structures using imperialist competitive algorithm. Computers and Structures, 88(21-22), 1220-1229. https://doi.org/10.1016/j.compstruc.2010.06.011.

Kawade, M. G., & Navale, A. V. (2019). Optimization of Pipe Rack by Study of Braced Bay. International Journal of Research in Engineering, Science and Management, 2(2).

Khajeh, A., Ghasemi, M. R., & Ghohani Arab, H. (2017). Hybrid Particle Swarm Optimization, Grid Search. International Journal of Optimization in Civil Engineering, 7(2), 171-189.

M. DRAKE, R., & J. WALTER, R. (2010). Design of Structural Steel Pipe Racks. Engineering Journal, 47, 241-252.

Mahallati, A., Ghasemi, M. R., & Ghohani Arab, H. (2018). OPTIMIZATION OF STEEL MOMENT FRAME BY A PROPOSED EVOLUTIONARY ALGORITHM. INTERNATIONAL JOURNAL OF OPTIMIZATION IN CIVIL ENGINEERING, 8(4), 511-524.

Mech, L. D. (1999). Alpha status, dominance, and division of labor in wolf packs. Canadian Journal of Zoology, 77, 1196-1203. https://doi.org/10.1139/z99-099.

Mirjalili, S., & Lewis, A. (2016). The Whale Optimization Algorithm. Advances in Engineering Software, 95, 51-67. https://doi.org/10.1016/j.advengsoft.2016.01.008.

Mirjalili, S., Mirjalili, S. M., & Lewis, A. (2014). Grey Wolf Optimizer. Advances in Engineering Software, 69, 46-61. https://doi.org/10.1016/j.advengsoft.2013.12.007.

Pezeshk, S., V. Camp, C., & Chen, D. (2000). Design of Nonlinear Framed Structures Using Genetic Optimization. Journal of Structural Engineering, 126(3), 382-388. https://doi.org/10.1061/(ASCE)0733-9445(2000)126:3(382)

Rajeev, S., & Krishnamoorthy, C. S. (1992). Discrete Optimization of Structures Using Genetic Algorithms. Journal of Structural Engineering, 118(5), 1233-1250. https://doi.org/10.1061/(ASCE)0733-9445(1992)118:5(1233).

Salama, M. I. (2013). New simple equations for effective length factors. HBRC Journal, 10(2), 156-159. https://doi.org/10.1016/j.hbrcj.2013.10.003.

Seismology, International Institute of Earthquake Engineering and structures Edition 4. (2023). Seismic Design Regulations Oil industry facilities and structures Edition 4. Vice President of Engineering, Research and Technology.

Shahiditabat, A., & Mirghaderi, R. (2013). Pipe and Pipe Rack Interaction. International Journal of Applied Science and Technology, 3(5), 39-44.

Talatahari, S., Gandomi, A. H., Yang, X.-S., & Deb, S. (2015). Optimum design of frame structures using the Eagle Strategy with Differential Evolution. Engineering Structures, 91, 16-25. https://doi.org/10.1016/j.engstruct.2015.02.026.

Talbi, E. G. (2009). Metaheuristics: From Design to Implementation. Wiley.

Togˇan, V. (2012). Design of planar steel frames using Teaching-Learning Based Optimization. Engineering Structures, 34, 225-232. https://doi.org/10.1016/j.engstruct.2011.08.035.

Zakian, P., Ordoubadi, B., & Alavi, E. (2021). Optimal Design of Steel Pipe Rack Structures Using PSO, GWO, and IGWO Algorithms. Advances in Structural Engineering, 24(11), 1-13. https://doi.org/10.1177/13694332211004116.

بهینه‌سازی سازه‌های پایپرک لوله فولادی در صنعت نفت با استفاده از الگوریتم‌های فرا اکتشافی

- روح الامین چترآذر[1]، حامد قوهانی عرب[2*]، محمود میری[3]

۱. ۱-دانشجوی کارشناسی ارشد، گروه مهندسی عمران، دانشکده مهندسی، دانشگاه سیستان و بلوچستان، زاهدان، ایران

۲. ۲-دانشیار، گروه مهندسی عمران، دانشکده مهندسی، دانشگاه سیستان و بلوچستان، زاهدان، ایران

۳. ۳-استاد، گروه مهندسی عمران، دانشکده مهندسی، دانشگاه سیستان و بلوچستان، زاهدان، ایران

(ایمیل نویسنده مسئول: ghohani@eng.usb.ac.ir)

چکیـــــــده

پایپرک‌های فولادی یکی از سازه‌های مهم در صنایع مختلف از جمله نفت و پتروشیمی هستند که برای انتقال سیالات، گازها و مواد شیمیایی، مورد استفاده قرار می‌گیرند. با توجه به کاربرد وسیع این نوع سازه‌ها در صنایع نفت و گاز، بهینه‌سازی آن‌ها از اهمیت ویژه‌ای برخوردار است. هدف این تحقیق، کاهش هزینه‌ی ساخت پایپرک‌های فولادی از طریق بهینه‌سازی وزن به صورت کاربردی با استفاده از الگوریتم‌های فرا ابتکاری گرگ خاکستری و نهنگ و همچنین مقایسه‌ی پاسخ‌های آن‌ها می‌باشد. در این پژوهش، الگوریتم‌های نامبرده به‌صورت خودکار و با استفاده از برنامه‌نویسی در محیط MATLAB توسعه یافته‌اند و از طریق ارتباط با نرم‌افزار ETABS، طراحی بهینه‌ی پایپرک‌های فولادی با رعایت قیود آیین‌نامه‌ای امکان‌پذیر می‌باشد. پژوهش حاضر با بهره‌گیری از الگوریتم‌های فرا ابتکاری و رعایت الزامات آیین‌نامه‌های طراحی، در پی ارائه راهکاری عملی برای طراحی بهینه و ایمن سازه‌های پایپرک فولادی است تا از این طریق هزینه‌های ساخت در صنعت نفت و گاز را کاهش دهد. کارکرد طرح پیشنهادی بر روی دو پایپرک فولادی با رعایت نکات طراحی، ارزیابی شده است. نتایج نشان می‌دهد که هر دو روش بهینه‌سازی فرا ابتکاری گرگ خاکستری و نهنگ، می‌توانند به‌عنوان یک ابزار کارآمد برای مهندسان، در دستیابی به طرح‌های اقتصادی مورد استفاده قرار بگیرند.

واژگان کلیدی: سازه پایپرک فولادی، بهینه‌سازی، الگوریتم‌های فرا ابتکاری، الگوریتم بهینه‌سازی گرگ خاکستری، الگوریتم بهینه‌سازی نهنگ